GEOLOGY OF THE NORTHERN TACONIC ALLOCHTHON: STRAIN VARIATION IN THRUST SHEETS, BRITTLE FAULTS, AND POSTRIFT DIKE EMPLACEMENT

by

Jean Crespi, Jennifer Cooper Boemmels, and Jessica Robinson
Geosciences, University of Connecticut, Storrs, CT 06269

INTRODUCTION

This field trip has three purposes: (1) to present a synthesis of structural and strain data for the Taconic slate belt, which lies in the northern part of the Giddings Brook thrust sheet in the Taconic allochthon, (2) to present an analysis of fault-slip data for postcleavage faults in the region, and (3) to present the results of work on mafic dikes in the Taconic lobe of the New England–Québec igneous province. The stops have been selected to illustrate the along-strike variation in structure and strain, to show representative postcleavage faults, and to include dikes in a variety of orientations. The data presented at the stops cover a region that extends for about 60 km along strike in the Giddings Brook thrust sheet, from Hubbardton, Vermont, in the north to Salem, New York, in the south (Figs. 1 and 2).

Emplacement of the Taconic allochthon took place during the Early to Late Ordovician Taconic orogeny. In the northeastern United States, the Taconic orogeny has traditionally been interpreted as resulting from the collision of a west-facing volcanic arc with the eastern margin of Laurentia (Bird and Dewey, 1970; Rowley and Kidd, 1981; Stanley and Ratcliffe, 1985). In this interpretation, emplacement of the Taconic allochthon occurred in a proforeland setting. New geochronological data, however, indicate that the orogeny involved several phases (Karabinos et al., 1998, 2017; Macdonald et al., 2014, 2017). During the first phase, a west-facing volcanic arc built on peri-Gondwanan basement collided with a fragment of a hyperextended eastern Laurentian margin. During the second phase, this composite ribbon terrane collided with Laurentia proper. Slab breakoff and a reversal of subduction polarity resulted in the establishment of an east-facing volcanic arc. During the third and final phase, the Taconic allochthon was emplaced. In this revised interpretation, emplacement of the Taconic allochthon occurred in a retroarc setting.

The eastern North American margin developed after Paleozoic contractional tectonics culminated in the formation of Pangea. Early Mesozoic rifting of Pangea was accompanied by the development of a system of rift basins of Late Triassic and Late Triassic–Early Jurassic age and by massive outpourings of basalt of the ~201 Ma central Atlantic magmatic province (CAMP). The extension direction during rifting was generally northwest–southeast (Withjack et al., 2012). In the northeastern United States, CAMP dikes trend northeast–southwest, consistent with the extension direction for rifting. Postrift magmatic bodies include the plutons and sheet intrusions of the Early Cretaceous New England–Québec (NEQ) igneous province (McHone, 1984; McHone and Butler, 1984). The origin of these intrusives has long been debated. They may be related to passage of the Great Meteor hotspot (Morgan, 1972; Sleep, 1990), edge-driven convection (Matton and Jébrak, 2009), opening of the North Atlantic Ocean (McHone and Butler, 1984), delamination of overthickened crust, or some combination of these mechanisms.

VARIATION IN STRUCTURE AND STRAIN IN THE NORTHERN GIDDINGS BROOK THRUST SHEET

In the 1970s and 80s, Bill Kidd and students at SUNY Albany produced detailed bedrock geologic maps of the Taconic slate belt (available at www.atmos.albany.edu/geology/webpages/SUNYATaconicGeologicalMaps.html). Together with the Bedrock Geologic Map of Vermont (Ratcliffe et al., 2011), these maps show that (1) regional-scale structures within this part of the northern Giddings Brook thrust sheet curve to define a salient and recess and (2) the thrust sheet plunges gently to the south such that shallower structural levels are exposed along strike from north to south. As a result, the Taconic slate belt provides opportunities to understand the way strain varies around map-view curves in orogenic belts and with distance from the base of a thrust sheet.

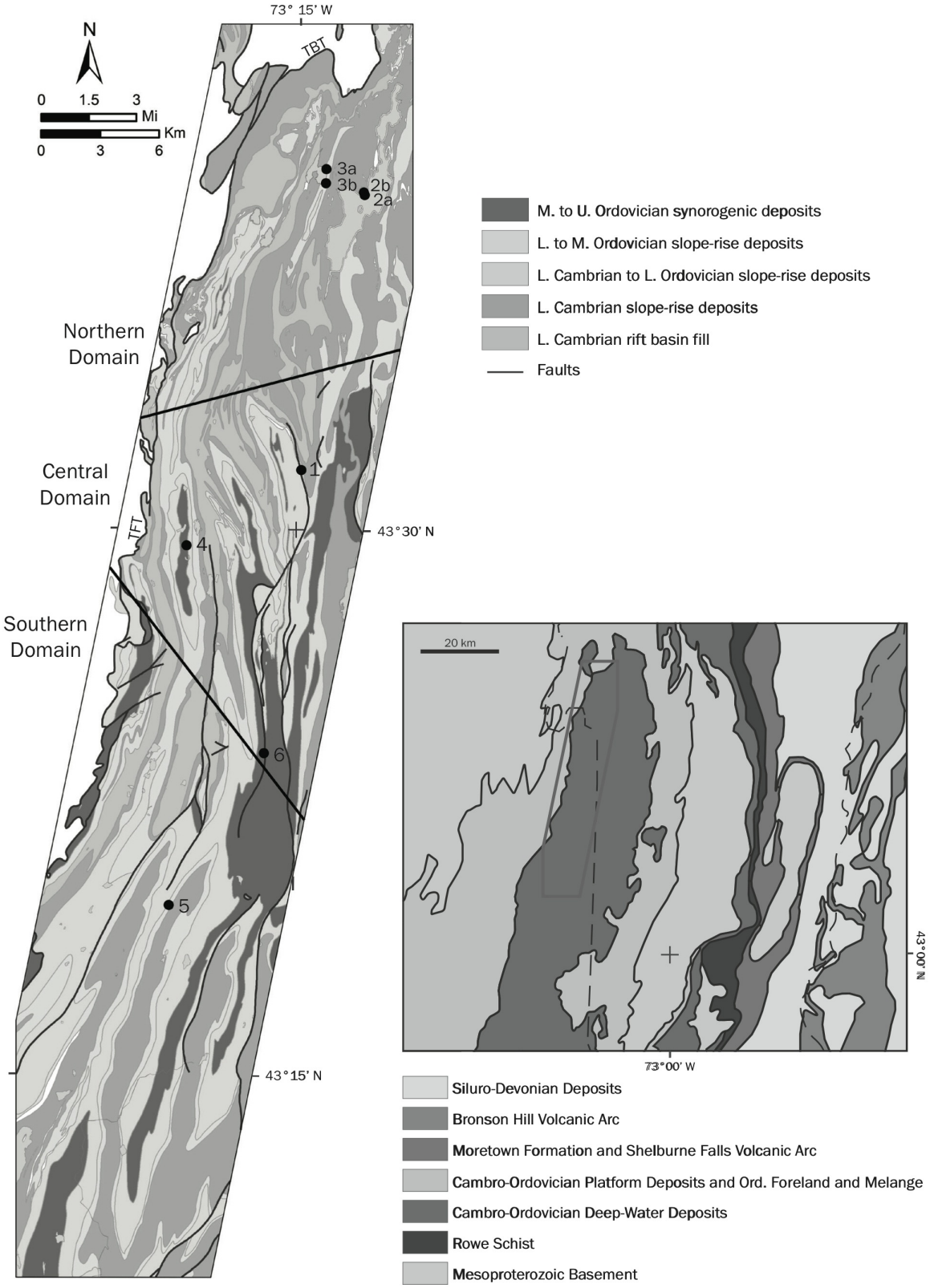

Figure 1. Bedrock geologic map of Taconic slate belt in northern part of Giddings Brook thrust sheet showing structural domains and field trip stops (modified from Ratcliffe et al. (2011); location map modified from Hibbard et al. (2006)).

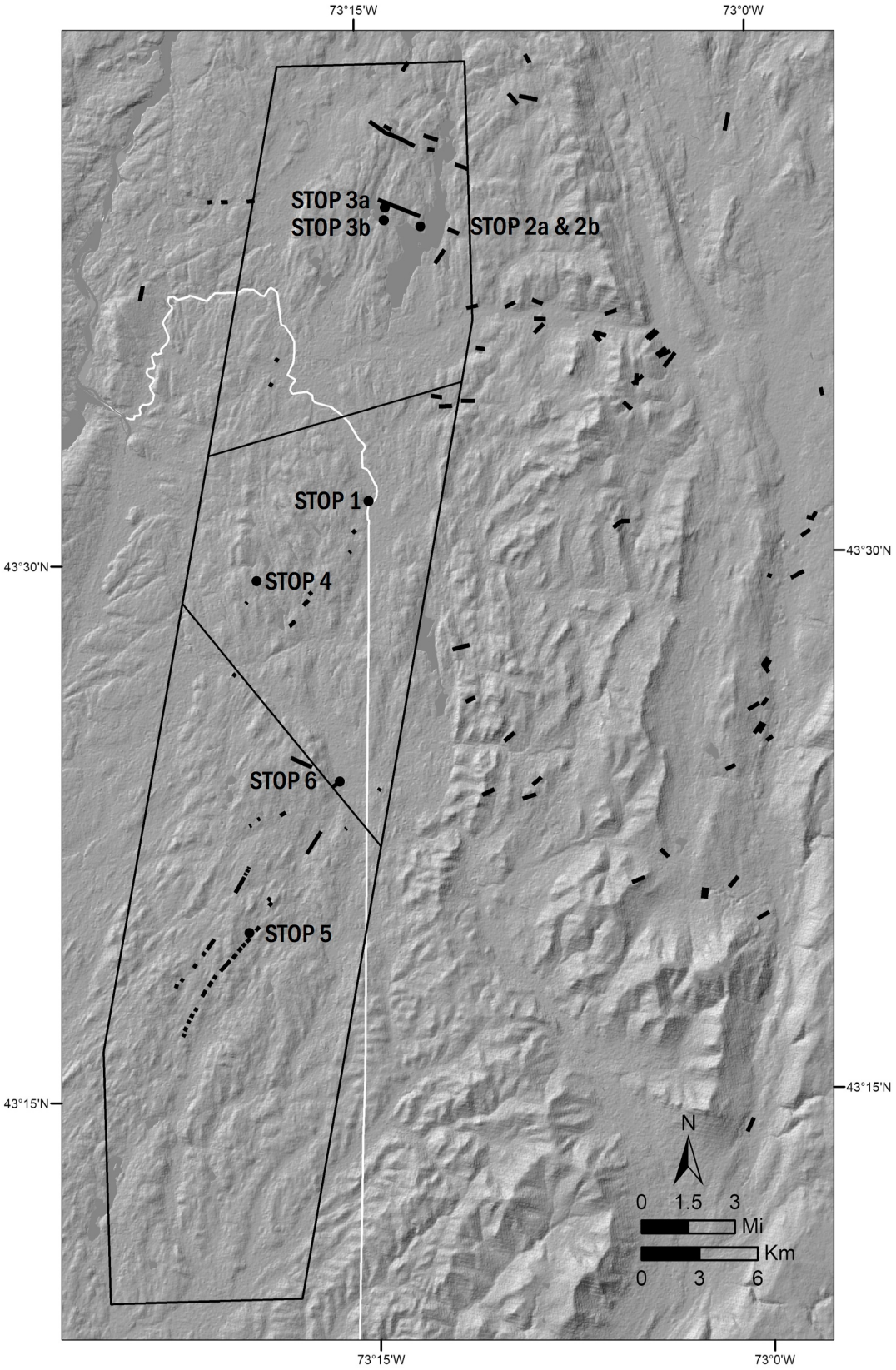

Figure 2. DEM of northern Taconic allochthon and vicinity showing dikes in Taconic lobe of NEQ igneous province and field trip stops (modified from Dale (1899), Fisher (1985), and Ratcliffe et al. (2011)).

The salient and recess are defined mainly by variations in the trend of the axial traces of regional-scale folds (Fig. 1). In Vermont, the axial traces trend north-northeast–south-southwest, parallel to the overall trend of the Taconic allochthon. Across the state border to the south in New York, the axial traces have north-northwest–south-southeast trends. Further south in New York, the axial traces return to north-northeast–south-southwest trending. This curvature delineates a salient in the north and a recess in the south.

A plunge to the south for the northern part of the Giddings Brook thrust sheet is indicated by the along-strike variation in age of exposed stratigraphic units and by the mapped location of the trace of the Taconic Basal thrust. The oldest unit of the Taconic sequence in the Giddings Brook thrust sheet, Cambrian (?) rift clastics of the Bomoseen Member of the Nassau Formation, is more extensively exposed in the north than in the south. In addition, the youngest units, synorogenic strata of the Middle to Upper Ordovician Indian River, Mount Merino, and Pawlet/Austin Glen formations, are not present in the north but are extensively exposed in the south. The trace of the Taconic Basal thrust forms the northern boundary of the Giddings Brook thrust sheet, consistent with the plunge direction given by the along-strike variation in age of exposed stratigraphic units. The variation in age of exposed stratigraphic units together with the total thickness of the Taconic sequence indicates a plunge to the south of about 1° to 2°.

We have recognized three main structural domains and one subdomain in the Taconic slate belt (Fig. 1). The northern limb of the salient forms the northern domain. The shared limb of the salient and recess forms the central domain. The southern limb of the recess forms the southern domain. The subdomain, which we refer to as the high strain subdomain, occupies a small area of the shared limb of the salient and recess on the eastern edge of the central domain. All three domains and the high strain subdomain contain evidence for top-to-west-northwest noncoaxial flow during slaty cleavage development, and we interpret slaty cleavage development as part of a continuum of deformation related to emplacement of the Taconic allochthon during the Taconic orogeny. Other aspects of the cleavage-related strain, however, are distinct in each domain/subdomain. The northern and southern domains are characterized by dip-slip thrusting, with the strain magnitude and degree of fiber asymmetry higher in the structurally lower northern domain. The central domain, in contrast, has been interpreted as a region of inclined transpression (Crespi et al., 2010). The high strain subdomain is distinct from the central domain because it is characterized by dip-slip thrusting in addition to a higher strain magnitude. Stop 1 of this field trip is in the high strain subdomain. Stops 2 and 3 are in the northern domain. Stops 4 and 5 are in the central domain and southern domain, respectively. Stop 6 lies near the boundary between the central and southern domains.

TACONIC LOBE OF THE NEW ENGLAND–QUÉBEC IGNEOUS PROVINCE

Drawing from a reconnaissance map produced by C.D. Walcott of Burgess Shale fame, T. Nelson Dale published the first bedrock geologic map of the entire Taconic slate belt (Dale, 1899). The map broadly differentiates Lower Cambrian and Lower Silurian (Ordovician) rocks of different compositions and shows the location and orientation of igneous dikes, now interpreted to belong to the NEQ igneous province.

The igneous dikes in the Taconic slate belt lie in the Taconic lobe (Fig. 2), the southernmost of three lobes on the western edge of the NEQ igneous province (McHone and Butler, 1984). The Taconic lobe differs from the Monteregian Hills lobe in southern Québec and the Burlington lobe in northern Vermont in that the dikes in the Taconic lobe show a wide range in orientation with a dominant north-northeast–south-southwest trend. The dikes in the Monteregian Hills lobe generally trend west-northwest–east-southeast, except where they form radial patterns around Early Cretaceous intrusive stocks, and the dikes in the Burlington lobe generally trend east–west (McHone, 1978). The Taconic lobe also differs from the Monteregian Hills lobe in that NEQ plutons are rare in the Taconic lobe. The Monteregian Hills lobe, in contrast, contains ten stocks that form a linear belt oriented parallel to the overall trend of the NEQ dikes in the lobe (McHone, 1984).

Most of the radiometric dates for the intrusives in the Taconic lobe are K–Ar ages. The dates are summarized in McHone and McHone (1993) and Eby and McHone (1997). Two dikes have been dated, both lying in the Taconic allochthon, and these yielded ages of 113 ± 4 Ma and 108 ± 4 Ma. These dikes trend east-northeast–west-southwest

and north-northeast–south-southwest. The Cuttingsville igneous complex in the Green Mountain massif and a nearby andesitic breccia yielded ages of 97 ± 8 Ma to 108 ± 1 Ma and 101 ± 2 Ma, respectively. The only $^{40}Ar/^{39}Ar$ date from NEQ intrusives in the Taconic lobe is a 100 ± 0.3 Ma age for the Cuttingsville igneous complex (Hubacher and Foland (1991) as referenced in McEnroe (1996)). These ages are younger for the most part than those obtained from intrusives in the Burlington and Monteregian Hills lobes (Foland et al., 1986; Bailey et al., 2017).

The NEQ intrusives in the Taconic lobe have received much less attention than the NEQ intrusives in the Burlington and Monteregian Hills lobes. We are currently obtaining new geochemical and geochronological data for the Taconic lobe intrusives to better define the similarities and differences between the three lobes and to improve understanding of the role of the NEQ igneous province in the postrift evolution of the eastern North American margin. We will examine NEQ dikes at Stops 3, 5, and 6 of this field trip.

POSTCLEAVAGE FAULTS

Mesoscale faults that postdate slaty cleavage development are relatively common in the Taconic slate belt. The orientation of many of these faults has been influenced by the orientation of slaty cleavage, the faults reactivating cleavage surfaces or striking parallel to but dipping more steeply than cleavage. The faults may also reactivate bedding surfaces, and, in some cases, they reactivate folded bedding such that the overall direction of fault slip is parallel to the fold hinge line. Other mesoscale, postcleavage faults in the Taconic slate belt, however, do not show evidence of having formed along preexisting surfaces.

Most of the mesoscale, postcleavage faults in the Taconic slate belt are normal faults or oblique- and strike-slip faults with a component of normal displacement. Faure et al. (1996, 2006) analyzed normal faults along strike in the Québec Appalachians and attributed the faults to two main extensional events: Late Triassic–Early Jurassic rifting of Pangea involving the separation of eastern North America and northwestern Africa and Early Cretaceous rifting of Pangea involving the separation of Labrador and Greenland. Paleostress analysis of faults interpreted as related to the former yielded east–west and northwest–southeast trends for the minimum compressive stress (Faure et al., 2006). Paleostress analysis of faults interpreted as related to the latter yielded an early phase of northeast–southwest extension and a later phase of north–south extension contemporaneous with emplacement of the intrusive bodies in the Monteregian Hills lobe of the NEQ igneous province (Faure et al., 1996). Separation of the normal faults into two main extensional events is facilitated in the Québec Appalachians by the difference in orientation for the minimum compressive stress indicated by the trends of CAMP and NEQ dikes.

Lim et al. (2005) analyzed mesoscale normal faults in the mélange belt west of the Taconic allochthon and attributed the faults to gravitational collapse of the Taconic orogenic wedge. The faults crosscut both the phacoidal cleavage in the mélange and postcleavage reverse faults related to slip along the Champlain thrust. They may or may not contain vein material. Crosscutting relations suggest the normal faults with vein material predate the normal faults without vein material. The normal faults are thought to have formed shortly after Taconic convergence ceased because fluid inclusions in the vein material yielded homogenization temperatures similar to or slightly lower than those obtained from fluid inclusions in vein material along the reverse faults and because the relatively high homogenization temperatures are inconsistent with an origin during a subsequent tectonic event.

The mesoscale, postcleavage normal faults in the Taconic slate belt may have formed during gravitational collapse of the Taconic orogenic wedge, during Late Triassic–Early Jurassic rifting of Pangea, and/or during emplacement of the Early Cretaceous dikes in the Taconic lobe of the NEQ igneous province. A gravitational collapse origin is supported by the Taconic allochthon lying closer to the hinterland of the Taconic orogenic wedge than the mélange belt to the west of the Taconic allochthon. A Late Triassic–Early Jurassic rifting origin is supported by evidence for rift-related normal faults several hundred kilometers west of the coast in the Québec Appalachians (Faure et al., 2006). An NEQ origin is supported by dike-fault crosscutting relations. In particular, a north-northeast-trending dike in the Taconic allochthon to the east of the Taconic slate belt is cut by a normal fault (Zen, 1972). The dike has yielded a hornblende K–Ar age of 108 ± 4 Ma (Zen, 1972; McHone and McHone, 1993).

Our analyses of mesoscale, postcleavage normal faults, oblique-slip faults, and strike-slip faults in the Taconic slate belt show that they are broadly consistent with east–west to northwest–southeast extension. Although NEQ dikes in the Taconic slate belt trend west-northwest–east-southeast and east–west, we have not identified normal faults indicative of north-northeast–south-southwest or north–south extension. We will examine mesoscale, post-cleavage faults at Stops 1, 4, and 6 of this field trip.

ROAD LOG

Meet on Sunday, October 14 at 8:30 a.m. at Stop 1 (43° 31.610'N, 73° 14.835'W). Park in the parking lot for the Ole Hampton House Tavern at 110 Campbell Lane in Hampton, New York. The restaurant does not have a sign other than "Free Pizza," "Band Sat. Night," or the like. It is located on the northeast corner of the intersection of County Road 18A and Campbell Lane. Park on the side of the parking lot near the trees away from the restaurant. Bring lunch and water. The lunch stop for this trip is at Glen Lake boat launch, and there is no place nearby to purchase lunch. Most of the stops are a short walk over relatively even terrain from the parking areas. One of the stops involves a scramble up a pile of slate rubble at the end of a short uphill walk into an abandoned quarry, and another stop is reached via a three-quarter mile round-trip walk in the woods on a relatively level portion of a marked hiking trail. Restrooms are available at the Stewart's Shops in Poultney (near Stop 1) and in Fair Haven (on the drive to Stop 2 and on the drive to Stop 4). Be prepared to catch up with the group on your own if you stop to use the restroom.

Mileage

0.0 Parking area for Stop 1. Stop 1 (43° 31.610'N, 73° 14.835'W) is the roadcut on either side of Co. Rd. 18A.

STOP 1. HIGH STRAIN SUBDOMAIN (POULTNEY/DEEP KILL FORMATION). 43° 31.610'N, 73° 14.835'W. (1 HOUR).

This exposure of the Lower to Middle Ordovician Poultney/Deep Kill Formation was created in the mid 1990s when County Road 18A was constructed to improve road traffic safety. The strata lie on the overturned limb of a regional-scale syncline and in the immediate footwall of the out-of-sequence Middle Granville thrust. Our analysis of the orientations of slaty cleavage and the stretching lineation and of syntectonic fibers places the exposure in the high strain subdomain on the eastern edge of the central domain.

Slaty cleavage strikes north-northeast and dips moderately east-southeast, and the stretching lineation plunges approximately down the dip of slaty cleavage. Syntectonic fibers associated with slaty cleavage development are curved in *XZ* sections consistent with top-to-west-northwest noncoaxial flow. The fibers yield stretch values for the *X* direction of about 2.2–2.3. They also record a small amount of extension in the *Y* direction. The central domain, in contrast, is characterized by north-northwest strikes for slaty cleavage, a moderately raking stretching lineation, and lower stretch values for the *X* direction.

Many mesoscale folds are present in the exposure (Fig. 3). They are unusual because the hinge lines plunge moderately to steeply southeast. Hinge lines of folds in the Taconic slate belt are typically subhorizontal to gently plunging, and, in the central domain, the plunge direction is south-southeast. The bedding-cleavage intersection lineation also plunges to the southeast although not as steeply as the fold hinge lines. This difference is likely because the mesoscale folds are mostly in the middle of the exposure and the bedding-cleavage intersection lineation was measured at the ends of the exposure where bedding is planar. The folds in the exposure are also asymmetrical such that they have an S shape when viewed down plunge.

The fold geometry can be explained by initial development of parasitic folds and subsequent rotation of the hinge lines of the parasitic folds toward the stretching lineation. The S-shaped fold asymmetry is consistent with an origin as parasitic folds on the overturned limb of a west-vergent, regional-scale fold. In addition, the orientation of

Figure 3. Photograph of asymmetric folds in middle of roadcut on northeast side of County Road 18A at Stop 1. View is to northeast.

the hinge lines is consistent with an initial gentle south-southeast plunge and counterclockwise rotation toward the downdip stretching lineation during top-to-west-northwest noncoaxial flow. This interpretation implies that this area was a long-lived region of high strain, the folds starting to rotate during folding and continuing to rotate during slaty cleavage development. The Middle Granville thrust may be a late-stage expression of this high strain zone.

Mesoscale, postcleavage faults in the strata typically contain laminated veins with well-developed steps. Some of the faults have formed along folded surfaces, a good example lying on the northeast side of County Road 18A near the middle of the exposure (Fig. 4). These faults are normal faults on the long limbs of the folds and reverse faults on the short limbs of the folds. Slip was subparallel to the hinge lines. In the example in Figure 4, the outer part of the fold has moved up relative to the inner part of the fold, and the striae show a systematic variation in orientation around the fold such that they are closer to exactly parallel to the hinge line in the hinge.

0.0 Turn left out of the parking area for Stop 1 onto Campbell Ln.
0.0 At the stop sign, turn right onto Co. Rd. 18A.
0.0 Pass Stop 1.
0.2 At the stop sign, turn right onto NY-22A.
3.0 Cross into Vermont. NY-22A becomes VT-22A.
4.5 VT-22A merges with VT-4A/Main St.
4.7 Pass the Fair Haven town green.
4.8 Keep to the right to continue on VT-4A/Main St.
5.2 At the 4-way stop, continue straight onto Dutton Ave.
5.6 Cross over US-4.
5.7 Dutton Ave. becomes Scotch Hill Rd.
9.0 Scotch Hill Rd. becomes West Castleton Rd.
9.6 Pass Stop 3b.

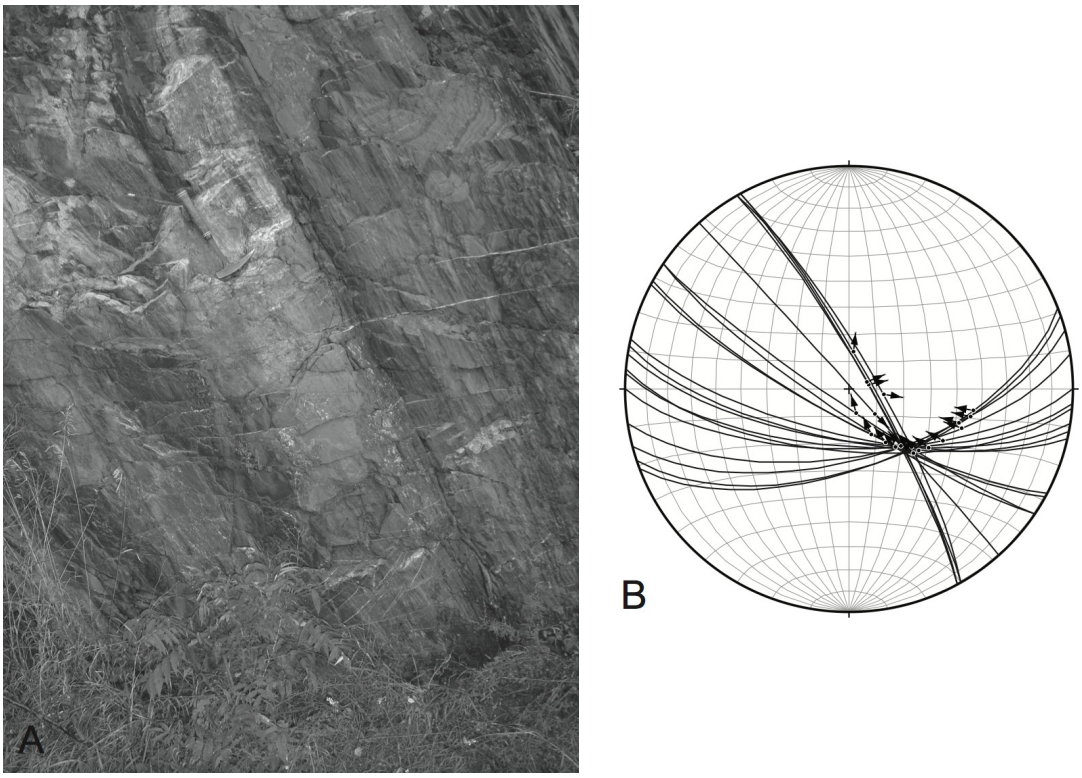

Figure 4. (A) Photograph of fold at Stop 1 (fold in bottom right of Fig. 3). View is to north-northwest. Handle of hammer is parallel to hinge line. (B) Stereonet of bedding-parallel faults in fold in (A). Great circles—fault planes; dots—striae; arrows—motion of hanging wall. Equal-area, lower-hemisphere projection.

9.6 Keep to the right to stay on the paved road (West Castleton Rd.).

9.8 Intersection of West Castleton Rd., Cedar Mountain Rd. (to the left), and the entrance to Bomoseen State Park (straight ahead). Turn left onto Cedar Mountain Rd. (dirt road).

11.0 Park at the entrance to Cedar Point quarry. Do not block access to the white house. Stop 2a (43° 39.185'N, 73° 12.525'W) is located a short distance from the start of the path into Cedar Point quarry, and Stop 2b (43° 39.255'N, 73° 12.555'W) is located at the top of the slate pile at the end of the path into the quarry.

The walk into Cedar Point quarry is relatively easy until the last part which involves climbing up a pile of slate rubble. Walk up the path to Stop 2a, which is to the right of the path near the beginning of the path. Continue walking up the path. At the Y, bear left onto a relatively level part of the path (do not take the uphill path to the right). At the end of the path, climb the pile of slate rubble to Stop 2b. Return to the path and follow it back to the entrance to the quarry.

STOP 2. NORTHERN DOMAIN (METTAWEE SLATE/MIDDLE GRANVILLE SLATE). 43° 39.185'N, 73° 12.525'W and 43° 39.255'N, 73° 12.555'W. (1 HOUR 15 MINUTES).

Cedar Point quarry exposes the hinge zone of a north-northeast-trending, regional-scale syncline. The folded strata belong to the Lower Cambrian Mettawee Slate/Middle Granville Slate, a purple and green slate that contains reduction spots useful for strain analysis. The quarry lies in the northern domain where slaty cleavage strikes north-northeast and dips gently east-southeast and where the stretching lineation plunges approximately down the dip of slaty cleavage. Here, slaty cleavage is overprinted by a crenulation cleavage, which becomes the dominant cleavage to the east of the approximate longitude of Lake Bomoseen and Lake St. Catherine. Although this crenulation cleavage is locally present in the Taconic slate belt, it does not appear to affect the orientation of slaty cleavage. In the northern domain, where the crenulation cleavage is more common than in the central and southern domains, the

mean orientation of slaty cleavage for sites without a crenulation cleavage is essentially the same as the mean orientation of slaty cleavage for sites with a weakly to moderately developed crenulation cleavage.

At Stop 2a, the concave side of a folded bedding surface is visible through the graffiti. The intersection of the axial planar slaty cleavage with bedding indicates the hinge line of the syncline is gently plunging, which is typical of folds in the Taconic slate belt. At Stop 2b, the convex side of a folded bedding surface and the profile plane of the syncline are visible. The tight to isoclinal nature of the syncline is typical of folds in the Taconic slate belt.

Reduction spots are common in the slabs in the slate pile at Stop 2b. Two types of reduction spots are present: those with irregular shapes and those that are elliptical. The latter have been measured and reported on by Wood (1974), Hoak (1992), and Goldstein et al. (1995). The reduction spots here and elsewhere in the Taconic slate belt plot in the flattening field of a Flinn plot, and Goldstein et al. (1995) interpreted their horizontal distribution on a Flinn plot as indicating the slates underwent a minimum of 55% volume loss during slaty cleavage development. Our strain data for the northern domain from strain fringes around pyrite framboids in black slates are not consistent with the reduction spot data. The strain fringes do not show fiber growth in the *Y* direction, and so we infer plane strain deformation for slaty cleavage development. In addition, the strain fringe data yield internally consistent data when combined with the orientation of slaty cleavage if constant volume is assumed. The 2.28 mean stretch value for the *X* direction obtained from strain fringes for the northern domain gives a strain ratio for the *XZ* plane of 5.2 for constant volume and a strain ratio for the *XZ* plane of 10.4 for 50% volume loss. These values can be plotted on an R_{XZ} versus θ' graph for simultaneous simple shear and volume change (Fossen and Tikoff, 1993) using the 28° mean dip of slaty cleavage in the northern domain and an appropriate dip for the Giddings Brook thrust sheet. We use a thrust sheet dip of 5° east, giving a θ' value of 23°. A value of 5.2 for R_{XZ} results in the northern domain plotting close to the curve for simple shear, which is by definition a constant volume deformation. A value of 10.4 for R_{XZ} results in the northern domain plotting in the volume gain field, which is at odds with the 50% volume loss assumption used to obtain R_{XZ}.

0.0 Return along Cedar Mountain Rd. to the intersection of Cedar Mountain Rd., West Castleton Rd., and the entrance to Bomoseen State Park.

1.2 Intersection of Cedar Mountain Rd., West Castleton Rd., and the entrance to Bomoseen State Park. At the stop sign, turn right onto West Castleton Rd.

1.3 At the Y, bear right onto Moscow Rd. (dirt road).

1.3 At the intersection, keep to the right to continue on Moscow Rd. toward Glen Lake boat launch.

1.4 Turn right into the parking area for Glen Lake boat launch and park. Walk back a short distance along Moscow Rd. to Glen Lake boat launch. Stop 3a (43° 39.885'N, 73° 13.980'W) is located on Glen Lake Trail about 10 minutes (~0.35 miles) from the trailhead. To access Glen Lake Trail, walk past the boulder barrier at the boat launch. Stop 3b (43° 39.500'N, 73° 13.995'W) is located in the backyard of the camp on West Castleton Rd. where the road passes Glen Lake. Stop 3b is a no-hammer stop.

Glen Lake Trail (visit vtstateparks.com/assets/pdf/bomoseentrailmap.pdf for a copy of the trail map) is well marked with blue trail blazes, and the walk to Stop 3a is relatively easy with little elevation change, the occasional fallen tree, and some irregular terrain where the trail passes over exposed tree roots. About 7 minutes (~0.25 miles) from the trailhead, the trail splits shortly after passing a foundation. Take the right fork, which passes on the east side of a cellar hole. The left fork follows the water's edge and is not the main trail. About 10 minutes (~0.35 miles) from the trailhead, the trail climbs up a small ridge. A hemlock tree with a girth of about 2 m and a blue trail blaze stands at the top of the ridge. The south-southwest side of the Bomoseen dike is exposed in the vicinity of this tree. Continue to follow the trail as it descends into a small valley to the north of the ridge. The valley is before the trail bends downhill to the left. Walk off trail just upslope from the valley floor to where a recently fallen tree has exposed the north-northeast side of the Bomoseen dike. Return to the trail and follow it downhill to the right. Rubble next to the trail of the dike and wall rock marks the dike-wall rock contact on the north-northeast side of the dike. Follow the trail up-

hill back to the valley floor and walk off trail to the east-southeast toward Moscow Rd. Several exposures of the dike and of the wall rock to the south-southwest of the dike are present in this area. Return to the trail and follow it back to the trailhead.

Walk back along Moscow Rd. and West Castleton Rd. to Stop 3b.

Return to Glen Lake boat launch. Lunch. Note the outcrops of the Poultney/Deep Kill Formation, which are on the gently dipping, upright limb of the Scotch Hill syncline.

STOP 3. BOMOSEEN DIKE AT GLEN LAKE (STOP 3A), NORTHERN DOMAIN (POULTNEY/DEEP KILL FORMATION) (STOP 3B), AND LUNCH. 43° 39.885'N, 73° 13.980'W and 43° 39.500'N, 73° 13.995'W. (2 HOURS).

The exposure of the Bomoseen dike at Stop 3a consists of several small and discontinuous outcrops of the dike between the eastern shore of Glen Lake and Moscow Road. Outcrops of the wall rock (West Castleton Formation on the Bedrock Geologic Map of Vermont (Ratcliffe et al., 2011) and Poultney and Hatch Hill formations on Rowley's map of the Lake Bomoseen area (Rowley, 1983, Plate 1)) are also present.

The Bomoseen dike was named by McHone and McHone (1993) for an exposure of the dike on VT-30 along the eastern shore of Lake Bomoseen. The dike appears on Dale's map of the Taconic slate belt (Fig. 5) (Dale, 1899) and is reproduced on Fowler's map of the Castleton area (Fowler, 1950, Plate II) and on the Bedrock Geologic Map of Vermont (Ratcliffe et al., 2011). It trends west-northwest–east-southeast and is relatively wide and long compared to other NEQ dikes in the Taconic lobe.

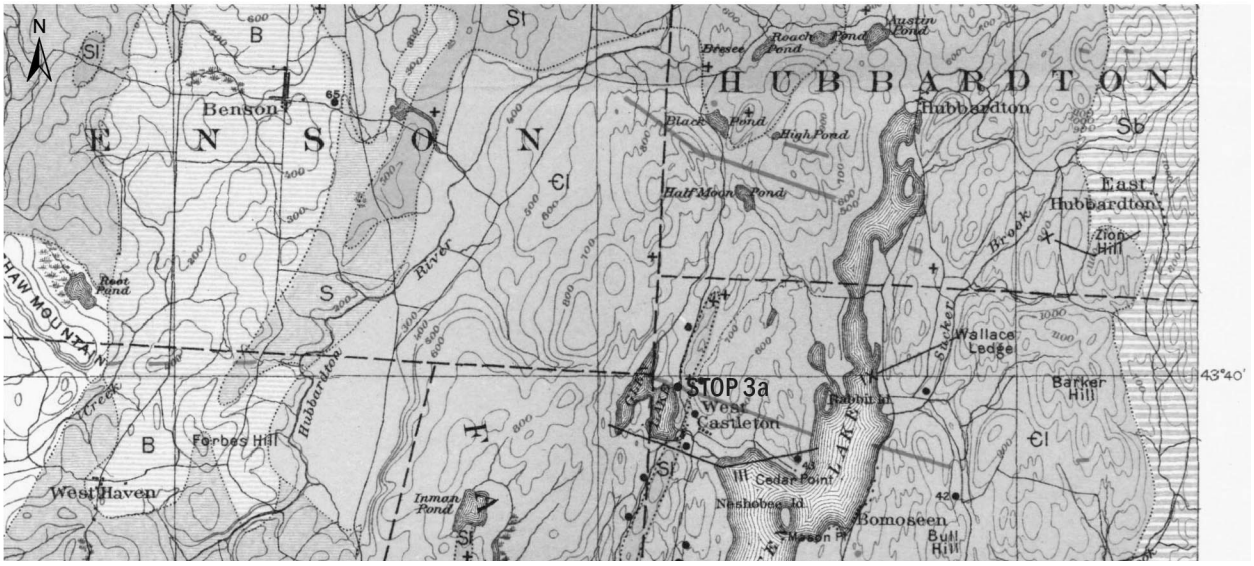

Figure 5. Portion of Dale's map of Taconic slate belt (Dale, 1899) showing location of Stop 3a. Map scale is 1:115,385.

McHone and McHone (1993) reported a width of 12 m for the Bomoseen dike at the VT-30 exposure (the entire width of the dike is no longer preserved). Our observations of the dike at the Glen Lake exposure give a comparable width. The location of the dike-wall rock contact on the north-northeast side of the dike can be located fairly closely on the trail by the change from dike rubble to slate rubble. A sample we collected from the southern side of the exposure of the dike closest to Moscow Road contains the dike-wall rock contact on the south-southwest side of the dike.

The Bomoseen dike is shown as extending continuously for nearly 5 km on Dale's map of the Taconic slate belt (Dale, 1899). In addition to the Glen Lake and VT-30 locations, the Bomoseen dike is well exposed along North Road.

Of interest at Stop 3a is the well-developed pencil cleavage in the wall rock adjacent to the dike-wall rock contact on the north-northeast side of the dike. This pencil cleavage has been formed by the intersection of the well-developed slaty cleavage with closely spaced dike-parallel fractures.

The exposure of the Scotch Hill syncline at Stop 3b (Fig. 6) is one of the best-known exposures in the Taconic slate belt. It lies in the northern domain. Slaty cleavage forms a divergent cleavage fan with the overall orientation of slaty cleavage similar to the mean orientation of slaty cleavage in the northern domain. Because sampling is prohibited at the exposure, the orientation of the stretching lineation was not determined, and the characteristics of strain fringes around subspherical core objects were not assessed.

Figure 6. Photograph of exposure of Scotch Hill syncline at Stop 3b. View is to northeast.

The folded strata, which belong to the Poultney/Deep Kill Formation, contain two sets of veins, one that predates folding and one that formed at the same time as folding. A subhorizontal, north-northeast-trending fold axis for the Scotch Hill syncline is shown by both the pole to the best-fit plane to the poles to bedding and by the bedding-cleavage intersection lineation at the exposure (Figs. 7A and 8A). The poles to slaty cleavage lie on the best-fit plane to the poles to bedding (Fig. 7A). The prefolding veins are similarly oriented throughout the fold, and their poles do not plot on the best-fit plane to the poles to bedding (Fig. 7B). The synfolding veins lie in a range of orientations, and their poles plot on the best-fit plane to the poles to bedding (Fig. 7B).

The prefolding veins are long, thin, and planar (Fig. 8B–D). They are commonly boudined (Fig. 8B), and they are crosscut by the synfolding veins (Fig. 8C, D). The synfolding veins have a less uniform morphology but are commonly short, thick, and sigmoidal (Fig. 8C–F). They are either boudined or folded depending on the angle between the vein and slaty cleavage. Synfolding veins that are especially thick, however, do not appear deformed. Although the prefolding veins appear approximately parallel to slaty cleavage on the profile plane of the fold, their noncoaxiality with the fold can be seen on west-northwest-facing bedding surfaces on the subvertical limb of the fold. The trace of cleavage on the bedding surfaces is subhorizontal whereas the trace of the prefolding veins plunges to the south. The coaxiality of the synfolding veins with the fold can also be seen on these surfaces. Both the trace of cleavage and the trace of the synfolding veins are subhorizontal (Fig. 8A).

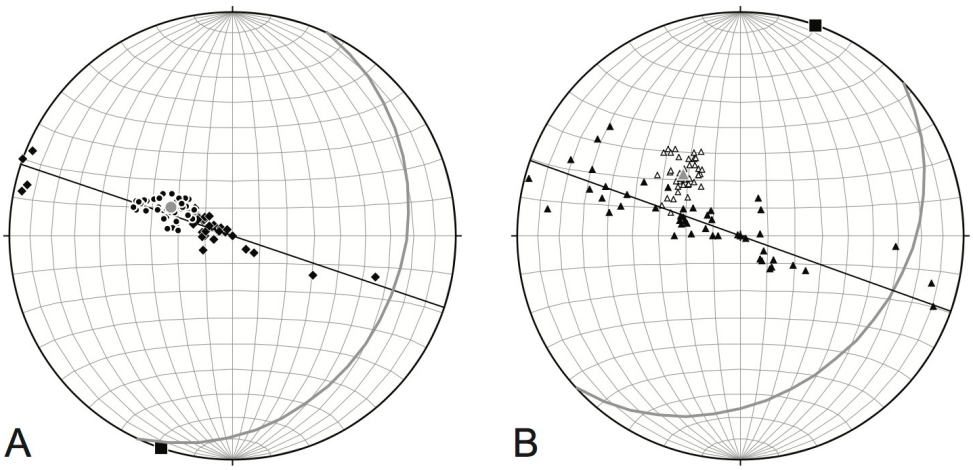

Figure 7. Stereonets of (A) bedding and slaty cleavage and (B) prefolding and synfolding veins at Stop 3b. Small black diamonds—poles to bedding; small black dots—poles to slaty cleavage; large gray dot—mean pole to slaty cleavage; small white triangles—poles to prefolding veins; small black triangles—poles to synfolding veins; large gray triangle—mean pole to prefolding veins; gray great circle—mean slaty cleavage in (A) and mean prefolding veins in (B); black great circle—best-fit plane to poles to bedding in (A) and best-fit plane to poles to synfolding veins in (B); large black square—fold axis given by pole to best-fit plane to poles to bedding in (A) and fold axis given by pole to best-fit plane to poles to synfolding veins in (B). Equal-area, lower-hemisphere projections.

The asymmetry of the synfolding veins is consistent with flexural folding. On the gently dipping limb of the fold, the synfolding veins are commonly irregularly shaped, but a large vein has a classic sigmoidal shape, the S shape when viewed to the north-northeast indicating thrust sense of shear (Fig. 8E). On the subvertical limb of the fold, the synfolding veins are commonly sigmoidal, the Z shape when viewed to the north-northeast indicating west-side-up sense of shear (Fig. 8F). These opposite senses of shear are as predicted for flexural folding with a pinned fold hinge. The mystery of the prefolding veins having similar orientations on the two limbs of the fold despite being prefolding is solved when shearing related to flexural folding is applied to their orientation. The change in orientation of the prefolding veins from limb rotation was essentially offset by the change in orientation from flexural-folding-related shearing within the bedding layers.

0.0 Turn left out of the parking area for Stop 3 onto Moscow Rd.
0.0 At the Y, bear right and continue on Moscow Rd.
0.1 At the yield sign, turn right onto West Castleton Rd.
0.1 Pass Stop 3b.
0.7 West Castleton Rd. becomes Scotch Hill Rd.
4.0 Scotch Hill Rd. becomes Dutton Ave.
4.1 Cross over US-4.
4.5 At the 4-way stop, continue straight onto VT-4A/N. Main St.
4.9 Pass the Fair Haven town green.
5.2 Turn right to continue on VT-4A/Prospect St.
6.6 At the stop sign/traffic light, turn left onto US-4.
6.8 Cross into New York.
8.7 Turn left onto Co. Rd. 21.
10.9 At the stop sign, continue straight on Co. Rd. 21.
12.7 Bear right onto Holcombville Rd.
14.4 Turn right onto Tanner Hill Rd.

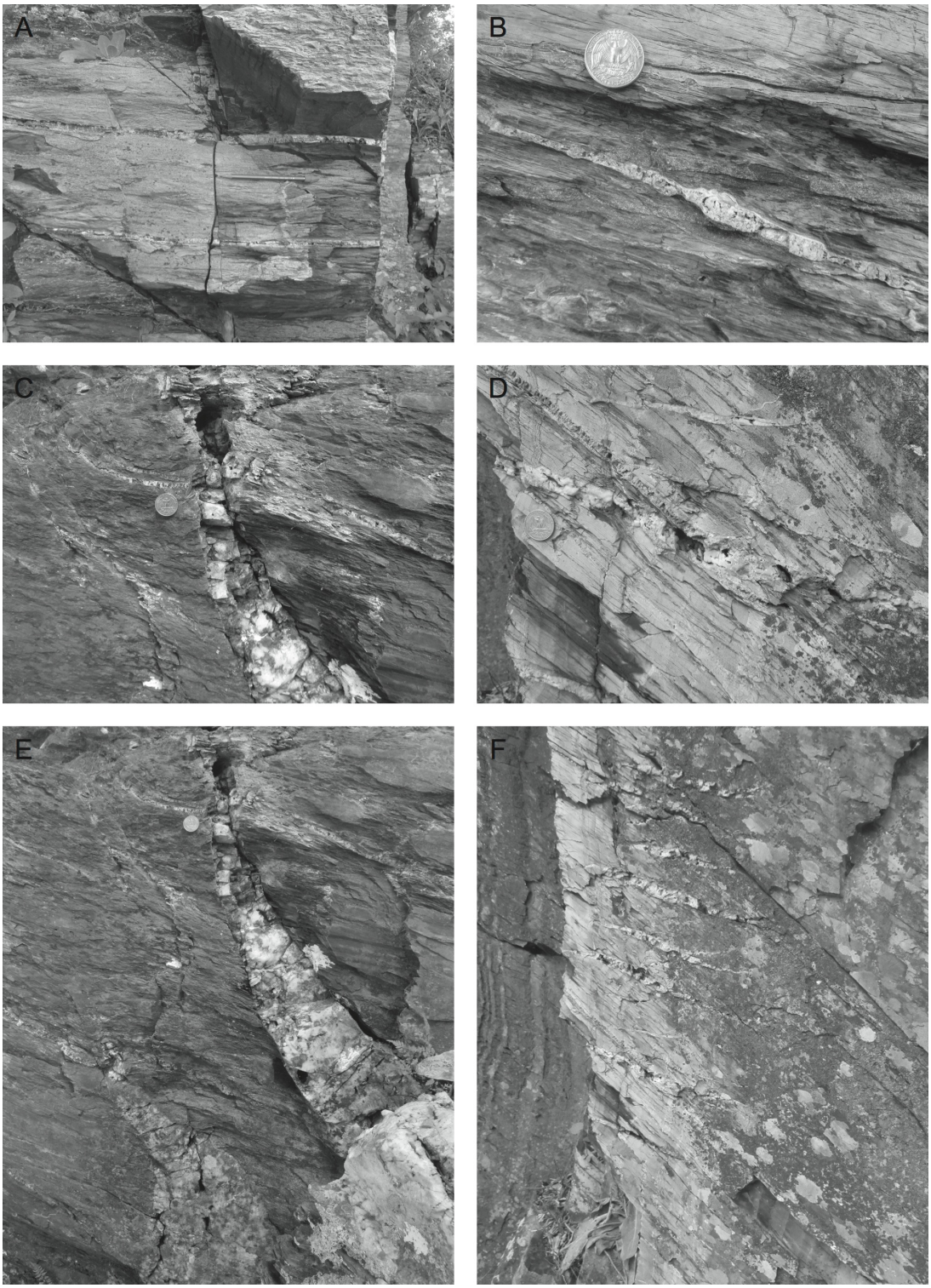

Figure 8. Photographs of structural features at Stop 3b. (A) Bedding surface on subvertical limb of fold. Pencil is horizontal and parallel to intersection of slaty cleavage on bedding and intersection of synfolding veins on bedding. (B) Prefolding vein on gently dipping limb of fold. (C) Crosscutting relation of prefolding and synfolding veins on gently dipping limb of fold. (D) Crosscutting relation of prefolding and synfolding veins on subvertical limb of fold. (E) S-shaped synfolding vein on gently dipping limb of fold. (F) Z-shaped synfolding veins on subvertical limb of fold. View is to east-southeast in (A). View is to north-northeast in (B)–(F).

15.1 Park on the shoulder on the northeast side of Tanner Hill Rd. Stop 4 (43° 29.515'N, 73° 19.125'W) is the quarry immediately east of the parking area and the exposures along the road in the vicinity of the parking area.

STOP 4. CENTRAL DOMAIN (INDIAN RIVER–PAWLET/AUSTIN GLEN FORMATIONS). 43° 29.515'N, 73° 19.125'W. (45 MINUTES).

The bedrock geology along Tanner Hill Road was mapped by Jacobi (1977) and is described in Rowley et al. (1979) and Landing (2002). The road transects the Tanner Hill syncline, and, although many of the exposures are small, the stratigraphic succession is readily observed and contacts between units are easily located. Exposures on the west limb of the syncline are somewhat inaccessible because of a new maple sugaring operation.

The small quarry immediately east of the parking area for this stop is in the Middle Ordovician Indian River Formation, a red slate interpreted as the oldest synorogenic unit in the Giddings Brook thrust sheet (Landing, 2002, 2012). Macdonald et al. (2017) dated a sample from a half-meter thick silicified layer of green slate in this quarry using LA-ICPMS and CA-IDTIMS. Zircon grains interpreted to be of primary volcanic origin and in the youngest population obtained by LA-ICPMS analysis yielded a CA-IDTIMS age of 466.06 ± 0.21 Ma.

Stop 4 lies in the central domain between the Taconic Frontal thrust and the Lee Road fault. The syncline extends for the length of the Taconic slate belt, the axial trace trending north-northeast–south-southwest in the northern and southern domains and north–south in the central domain. Folds between the Lee Road fault and Middle Granville thrust in the central domain have axial traces that trend north-northwest–south-southeast. The anomalous orientation of the fold axial traces is interpreted to be a result of the central domain having undergone inclined transpression (Crespi et al., 2010). Consistent with such a three-dimensional deformation, the stretching lineation is not downdip, and the strain fringes record extension in the *Y* direction. Moreover, in addition to the top-to-west-northwest sense of shear given by fibers in strain fringes in the *XZ* plane throughout the Taconic slate belt, fibers in strain fringes in the central domain are locally curved in the *XY* plane, the sense of curvature indicating sinistral shear.

Mesoscale, postcleavage normal faults are present in the exposures along Tanner Hill Road, most commonly in the Indian River Formation. Some of the faults contain laminated quartz and chlorite veins, but most lack fault-zone vein material, most likely because the faults are weathered. Faults with thick panels of laminated quartz and chlorite veins and well-developed steps can be found in out-of-place blocks in the quarries on either side of Tanner Hill Road. Although some faults are parallel to slaty cleavage, most strike parallel to but dip more steeply than cleavage (Fig. 9). The angle between the faults and slaty cleavage is on average about 10°–15°.

0.0 Continue on Tanner Hill Rd.
0.6 Intersection of Tanner Hill Rd., Truthville Rd., and Welch Rd. (to the right). Continue straight onto Truthville Rd.
2.6 At the stop sign, continue straight on Truthville Rd.
3.7 At the stop sign, continue straight onto Co. Rd. 12.
3.9 At the stop sign, turn right to continue on Co. Rd. 12A.
4.2 At the stop sign, turn right onto NY-22.
5.2 Bear left onto Co. Rd. 17.
5.8 At the stop sign, turn left onto NY-40.
12.0 At the traffic light, turn left onto NY-149.
15.8 Turn right onto Searles Rd. (dirt road).
16.6 At the stop sign, continue straight onto Liebig Rd.
16.8 View to the east of the Taconic Range and Green Mountains.
19.2 Turn right onto Big Burch Hill Rd.
19.4 Turn left onto Bardin Rd. (dirt road). Bardin Rd. is incorrectly labeled on Google Maps and Google Earth. Bardin Rd. is the road between Liebig Rd. to the east and "Bardin Rd." (a driveway) to the west.

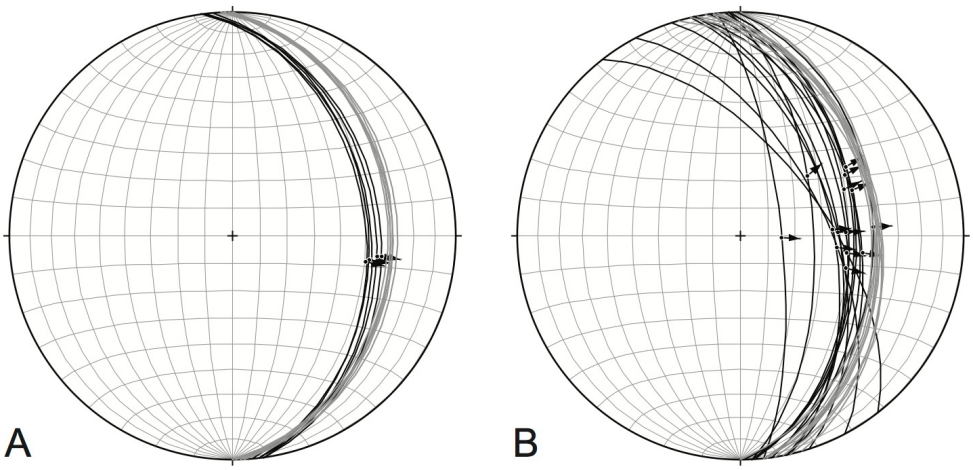

Figure 9. Stereonets of postcleavage faults and slaty cleavage in exposures of Indian River Formation along Tanner Hill Road. (A) Upright limb and (B) overturned limb of Tanner Hill syncline. Black great circles—fault planes; dots—striae; arrows—motion of hanging wall; gray great circles—slaty cleavage. Equal-area, lower-hemisphere projections.

19.4 Park along the west side of Bardin Rd. Walk a short distance along Bardin Rd. to the large bend in the road. Stop 5 (43° 19.630'N, 73° 19.670'W) consists of the small roadcuts along the west side of Bardin Rd. and various outcrops in the woods immediately west of Bardin Rd.

STOP 5. SOUTHERN DOMAIN (HATCH HILL FORMATION) AND BARDIN DIKE. 43° 19.630'N, 73° 19.670'W. (45 MINUTES).

This exposure of the Lower Cambrian to Lower Ordovician Hatch Hill Formation consists of interbedded black slate and quartz arenites. Subvertical bedding is visible in the small roadcut on the north side of the large bend in Bardin Road, and subhorizontal bedding is visible in the small roadcut on the south side of the large bend in Bardin Road. Subvertical to steeply east-dipping and subhorizontal bedding is visible in the outcrops in the woods immediately west of Bardin Road. The exposure lies on the upright limb of a regional-scale syncline on Shaw's map of portions of the Granville, Hartford, Hebron, and Pawlet townships (Shaw, 1984) and on the overturned limb of a regional-scale syncline on the Bedrock Geologic Map of Vermont (Ratcliffe et al., 2011). The bedding-cleavage relations at the exposure indicate a north-northeast-trending anticlinal hinge between the area with subvertical to steeply east-dipping bedding and the area with subhorizontal bedding. This anticline is parasitic to the regional-scale fold.

The characteristics of Stop 5 are typical of the southern domain. Slaty cleavage strikes north-northeast and dips about 30° east. The stretching lineation is about down the dip of slaty cleavage. Syntectonic fibers associated with slaty cleavage development are generally straight in *XZ* sections. Where they exhibit subtle curvature, the sense of curvature is consistent with top-to-west-northwest noncoaxial flow. The fibers yield a mean stretch value for the *X* direction of 1.6 and a mean stretch value for the *Y* direction of 1.1. The main differences between the southern and northern domains are that the fibers in the southern domain are not as curved as they are in the northern domain and that the stretch values for the *X* direction in the southern domain are not as high as they are in the northern domain. These differences are consistent with the southern domain lying at a higher structural level, i.e., farther from the base of the Giddings Brook thrust sheet, than the northern domain.

An igneous dike, which we have named the Bardin dike, lies in the hinge zone of the anticline indicated by the bedding-cleavage relations at the exposure (Fig. 10). This dike together with many of the other dikes/dike segments in the southern part of the Taconic lobe was mapped in 1895 by Florence Bascom, a pioneer in the advancement of women in geology. Bascom's work contributed to Dale's efforts to map the Taconic slate belt, and the dikes that she mapped appear on Dale's map of the Taconic slate belt (Dale, 1899). The Bardin dike is about 2 m wide. Its trend is

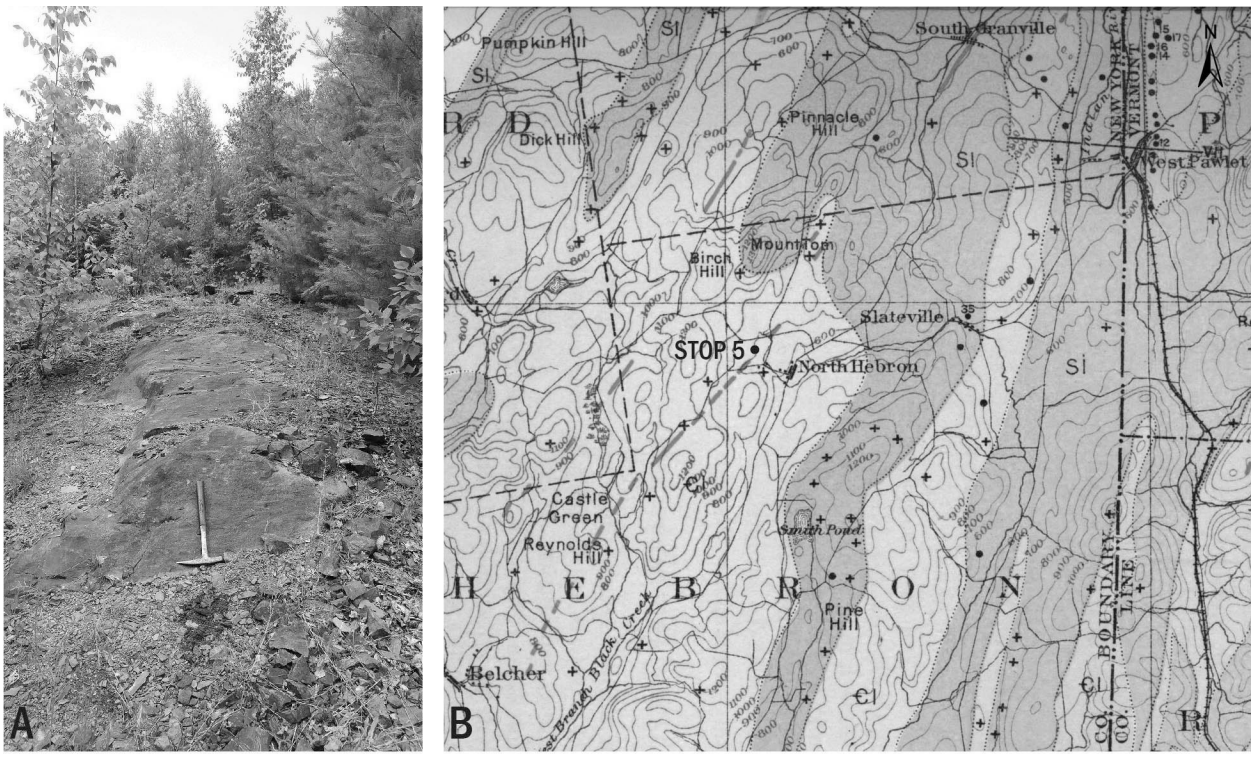

Figure 10. (A) Photograph of Bardin dike at Stop 5. View is to south-southwest. (B) Portion of Dale's map of Taconic slate belt (Dale, 1899) showing location of Stop 5. Map scale is 1:115,385.

subparallel to the axial traces of the regional-scale folds in the southern domain and to the axial trace of the local anticline that it has intruded. Like the Bomoseen dike, a well-developed pencil cleavage is present in the wall rock adjacent to the dike. It can be observed on both sides of the dike and has been formed by the intersection of the well-developed slaty cleavage with closely spaced dike-parallel fractures. Bascom's mapping shows the Bardin dike as one of a series of discontinuous dike segments that extends for about 12 km from Belcher, New York, to South Granville, New York (Fig. 10).

0.0 Continue on Bardin Rd.
0.3 Turn left at the T intersection onto Little Burch Hill Rd. (dirt road).
0.5 Bear right onto Liebig Rd.
0.8 At the stop sign, turn left onto Co. Rd. 31.
1.3 Turn left onto Co. Rd. 28.
4.8 At the stop sign, continue straight onto NY-149.
6.6 At the traffic light, turn left onto NY-149/NY-22.
6.7 Bear left to continue on NY-22.
7.0 Park on the shoulder on the northeast side of NY-22. Stop 6 (43° 23.825'N, 73° 16.150'W) is the roadcut on the northeast side of NY-22.

STOP 6. CENTRAL DOMAIN/SOUTHERN DOMAIN BOUNDARY (MOUNT MERINO FORMATION) AND GRANVILLE DIKE. 43° 23.825'N, 73° 16.150'W. (30 MINUTES).

This exposure of the Middle to Upper Ordovician Mount Merino Formation changes from interbedded black slate and chert in the northwestern part of the exposure to mainly chert in the southeastern part of the exposure. Slaty cleavage, which is well developed in the northwestern part of the exposure, dips moderately east, and bedding is subvertical. The exposure lies on the upright limb of a regional-scale anticline on Kidd's map of the Lee Road area

(Kidd, 1976)/Fisher's map of the Glens Falls–Whitehall region (Fisher, 1985) and on the Bedrock Geologic Map of Vermont (Ratcliffe et al., 2011). The bedding-cleavage relations here, however, indicate the exposure is on an overturned limb. This implies the strata are on the limb of a fold that is parasitic to the regional-scale fold.

Stop 6 lies near the boundary between the central and southern domains where the trend of the fold axial traces changes from north-northwest–south-southeast in the central domain to north-northeast–south-southwest in the southern domain. Slaty cleavage strikes slightly east of north and dips moderately east. The stretching lineation is about down the dip of slaty cleavage. We have not analyzed syntectonic fibers at this location.

A narrow igneous dike lies near the southeastern end of the exposure. This dike does not appear on Dale's map of the Taconic slate belt (Dale, 1899). It is shown, however, on Kidd's map of the Lee Road area (Kidd, 1976) and is reproduced on Fisher's map of the Glens Falls–Whitehall region (Fisher, 1985). We have named this dike the Granville dike. It is about 25 cm wide and has been mapped for a distance of about 0.4 km.

Like the Bardin dike, the Granville dike is one of a number of northeast-trending dikes/dike segments in the southern part of the Taconic lobe. These dikes have the same general trend in the southern domain, where the structural grain trends north-northeast–south-southwest, and in the central domain, where the structural grain trends north-northwest–south-southeast. Thus, while the dikes generally follow the structural grain in the southern domain, they cut across it in the central domain. The northeast-trending Granville dike cuts across the structural grain, but this is not immediately apparent at Stop 6 because both the dike and bedding are subvertical and because the orientation of bedding is difficult to see in three dimensions in the chert layers next to the dike. About 2 m to the northwest of the dike, bedding strikes about 035–040 (Fig. 11). Because the dike is slightly magnetic and somewhat curved, we used the orientation of dike-parallel fractures in the vicinity of the dike as a proxy for the orientation of the dike. These fractures strike about 060–075 (Fig. 11), which is oblique to bedding and similar to the 055–060 trend of the dike shown on Kidd's map of the Lee Road area (Kidd, 1976). The oblique relation between the Granville dike and the structural grain is readily seen on Kidd's map of the Lee Road area (Kidd, 1976)/Fisher's map of the Glens Falls–Whitehall region (Fisher, 1985) where the dike is shown cutting across the contact between the Indian River and Mount Merino formations (Fig. 11).

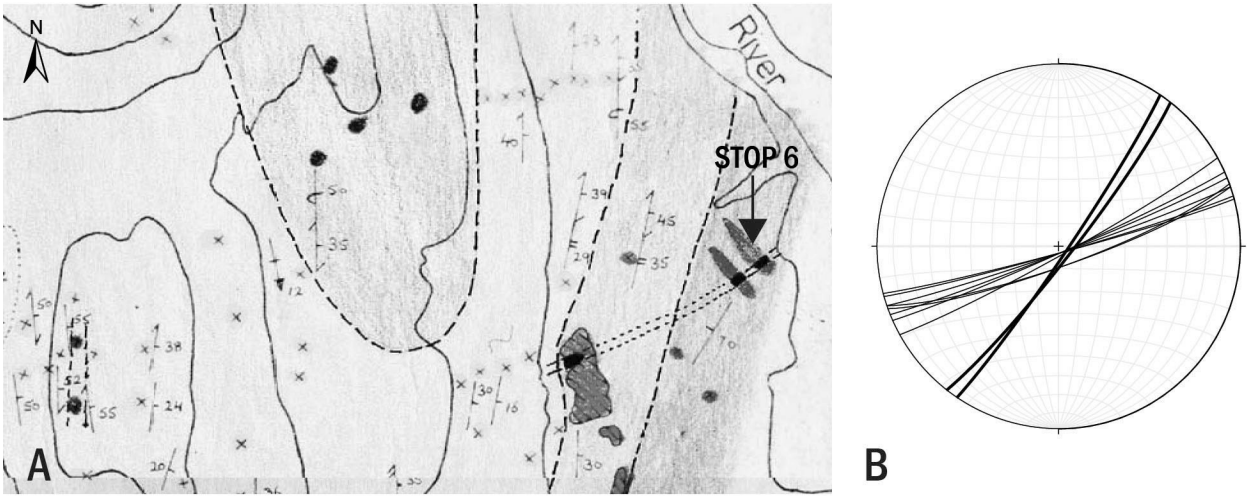

Figure 11. (A) Portion of bedrock geologic map of Lee Road area (Kidd, 1976) showing location of Stop 6. Stratigraphic units outward from core of anticline—Hatch Hill Formation, Poultney/Deep Kill Formation, Indian River Formation, Mount Merino Formation; black areas within parallel dotted lines—Granville dike. Map scale is 1:12,000. (B) Stereonet of bedding and dike-parallel fractures at Stop 6. Thick great circles—bedding; thin great circles—dike-parallel fractures. Equal-area, lower-hemisphere projection.

Several brittle faults are present in this exposure. They are either oblique to both bedding and slaty cleavage or parallel to bedding.

REFERENCES CITED

Bailey, D.G., Lupulescu, M., Chiarenzelli, J., and Traylor, J.P., 2017, Age and origin of the Cannon Point syenite, Essex County, New York: Southernmost expression of Monteregian Hills magmatism?: Canadian Journal of Earth Sciences, v. 54, no. 4, p. 379–392, https://doi.org/10.1139/cjes-2016-0144.

Bird, J.M., and Dewey, J.F., 1970, Lithosphere plate-continental margin tectonics and the evolution of the Appalachian orogen: Geological Society of America Bulletin, v. 81, no. 4, p. 1031–1060, https://doi.org/10.1130/0016-7606(1970)81[1031:LPMTAT]2.0.CO;2.

Crespi, J.M., Underwood, H.R., and Chan, Y.-C., 2010, Orogenic curvature in the northern Taconic allochthon and its relation to footwall geometry, *in* Tollo, R.P., Bartholomew, M.J., Hibbard, J.P., and Karabinos, P.M., eds., From Rodinia to Pangea: The lithotectonic record of the Appalachian region: Geological Society of America Memoir 206, p. 111–122, https://doi.org/10.1130/2010.1206(06).

Dale, T.N., 1899, The slate belt of eastern New York and western Vermont: U.S. Geological Survey Annual Report 19, pt. 3, p. 153–307.

Eby, G.N., and McHone, J.G., 1997, Plutonic and hypabyssal intrusions of the Early Cretaceous Cuttingsville complex, Vermont, *in* Grover, T.W., Mango, H.N., and Hasenohr, E.J., eds., Guidebook for the 89th Annual Meeting of the New England Intercollegiate Geological Conference: Castleton, Vermont, Castleton State College, p. B2-1–B2-16.

Faure, S., Tremblay, A., and Angelier, J., 1996, State of intraplate stress and tectonism of northeastern America since Cretaceous times, with particular emphasis on the New England–Québec igneous province: Tectonophysics, v. 255, no. 1–2, p. 111–134, https://doi.org/10.1016/0040-1951(95)00113-1.

Faure, S., Tremblay, A., Malo, M., and Angelier, J., 2006, Paleostress analysis of Atlantic crustal extension in the Québec Appalachians: The Journal of Geology, v. 114, no. 4, p. 435–448, https://doi.org/10.1086/504178.

Fisher, D.W., 1985, Bedrock geology of the Glens Falls–Whitehall region, New York: New York State Museum Map and Chart Series 35, scale 1:48,000, 3 sheets, 58 p. text.

Foland, K.A., Gilbert, L.A., Sebring, C.A., and Chen, J.-F., 1986, $^{40}Ar/^{39}Ar$ ages for plutons of the Monteregian Hills, Québec: Evidence for a single episode of Cretaceous magmatism: Geological Society of America Bulletin, v. 97, no. 8, p. 966–974, https://doi.org/10.1130/0016-7606(1986)97<966:AAFPOT>2.0.CO;2.

Fossen, H., and Tikoff, B., 1993, The deformation matrix for simultaneous simple shearing, pure shearing, and volume change, and its application to transpression-transtension tectonics: Journal of Structural Geology, v. 15, no. 3–5, p. 413–422, https://doi.org/10.1016/0191-8141(93)90137-Y.

Fowler, P., 1950, Stratigraphy and structure of the Castleton area, Vermont: Vermont Geological Survey Bulletin 2, 83 p.

Goldstein, A., Pickens, J., Klepeis, K., and Linn, F., 1995, Finite strain heterogeneity and volume loss in slates of the Taconic allochthon, Vermont, U.S.A.: Journal of Structural Geology, v. 17, no. 9, p. 1207–1216, https://doi.org/10.1016/0191-8141(95)00022-6.

Hibbard, J.P., van Staal, C.R., Rankin, D.W., and Williams, H., 2006, Lithotectonic map of the Appalachian orogen, Canada–United States of America: Geological Survey of Canada "A" Series Map 2096A, scale 1:1,500,000, 2 sheets, https://doi.org/10.4095/221912.

Hoak, T.E., 1992, Strain analysis, slaty cleavage, and thrusting in the Taconic slate belt: Northeastern Geology, v. 14, p. 7–14.

Hubacher, F.A., and Foland, K.A., 1991, $^{40}Ar/^{39}Ar$ ages for Cretaceous intrusions of the White Mountain magma series, northern New England, and their tectonic implications: Geological Society of America Abstracts with Programs, v. 23, p. 47.

Jacobi, L.D., 1977, Stratigraphy, depositional environment, and structure of the Taconic allochthon, central Washington County, New York [M.S. thesis]: Albany, New York, State University of New York at Albany, 191 p.

Karabinos, P., Samson, S.D., Hepburn, J.C., and Stoll, H.M., 1998, Taconian orogeny in the New England Appalachians: Collision between Laurentia and the Shelburne Falls arc: Geology, v. 26, no. 3, p. 215–218, https://doi.org/10.1130/0091-7613(1998)026<0215:TOITNE>2.3.CO;2.

Karabinos, P., Macdonald, F.A., and Crowley, J.L., 2017, Bridging the gap between the foreland and hinterland I: Geochronology and plate tectonic geometry of Ordovician magmatism and terrane accretion on the Laurentian margin of New England: American Journal of Science, v. 317, no. 5, p. 515–554, https://doi.org/10.2475/05.2017.01.

Kidd, W.S.F., 1976, Geology of the Lee Road area, Granville, New York: http://www.atmos.albany.edu/geology/webpages/SUNYATaconicGeologicalMaps.html (August 2018).

Landing, E., 2002, Early Paleozoic sea levels and climates: New evidence from the east Laurentian shelf and slope, *in* McLelland, J., and Karabinos, P., eds., Guidebook for the 94th Annual Meeting of the New England Intercollegiate Geological Conference and the 74th Annual Meeting of the New York State Geological Association: Lake George, New York, p. B6-1–B6-22.

Landing, E., 2012, The great American carbonate bank in eastern Laurentia: Its births, deaths, and linkage to paleooceanic oxygenation (Early Cambrian–Late Ordovician), *in* Derby, J.R., Fritz, R.D., Longacre, S.A., Morgan, W.A., and Sternbach, C.A., eds., The great American carbonate bank: The geology and economic resources of the Cambrian–Ordovician Sauk megasequence of Laurentia: American Association of Petroleum Geologists Memoir 98, p. 451–492, https://doi.org/10.1306/13331502M983502.

Lim, C., Kidd, W.S.F., and Howe, S.S., 2005, Late shortening and extensional structures and veins in the western margin of the Taconic orogen (New York to Vermont): The Journal of Geology, v. 113, no. 4, p. 419–438, https://doi.org/10.1086/430241.

Macdonald, F.A., Ryan-Davis, J., Coish, R.A., Crowley, J.L., and Karabinos, P., 2014, A newly identified Gondwanan terrane in the northern Appalachian Mountains: Implications for the Taconic orogeny and closure of the Iapetus Ocean: Geology, v. 42, no. 6, p. 539–542, https://doi.org/10.1130/G35659.1.

Macdonald, F.A., Karabinos, P.M., Crowley, J.L., Hodgin, E.B., Crockford, P.W., and Delano, J.W., 2017, Bridging the gap between the foreland and hinterland II: Geochronology and tectonic setting of Ordovician magmatism and basin formation on the Laurentian margin of New England and Newfoundland: American Journal of Science, v. 317, no. 5, p. 555–596, https://doi.org/10.2475/05.2017.02.

Matton, G., and Jébrak, M., 2009, The Cretaceous peri-Atlantic alkaline pulse (PAAP): Deep mantle plume origin or shallow lithospheric breakup?: Tectonophysics, v. 469, no. 1–4, p. 1–12, https://doi.org/10.1016/j.tecto.2009.01.001.

McEnroe, S.A., 1996, North America during the Lower Cretaceous: New paleomagnetic constraints from intrusions in New England: Geophysical Journal International, v. 126, no. 2, p. 477–494, https://doi.org/10.1111/j.1365-246X.1996.tb05304.x.

McHone, J.G., 1978, Distribution, orientations, and ages of mafic dikes in central New England: Geological Society of America Bulletin, v. 89, no. 11, p. 1645–1655, https://doi.org/10.1130/0016-7606(1978)89<1645:DOAAOM>2.0.CO;2.

McHone, J.G., 1984, Mesozoic igneous rocks of northern New England and adjacent Québec: Geological Society of America Map and Chart Series MC-49, scale 1:690,000, 1 sheet, 5 p. text.

McHone, J.G., and Butler, J.R., 1984, Mesozoic igneous provinces of New England and the opening of the North Atlantic Ocean: Geological Society of America Bulletin, v. 95, no. 7, p. 757–765, https://doi.org/10.1130/0016-7606(1984)95<757:MIPONE>2.0.CO;2.

McHone, J.G., and McHone, N.W., 1993, Field guide to Cretaceous intrusions in the northern Taconic Mountains region, Vermont: Vermont Geology, v. 7, p. 1–27.

Morgan, W.J., 1972, Deep mantle convection plumes and plate motions: American Association of Petroleum Geologists Bulletin, v. 56, no. 2, p. 203–213, https://doi.org/10.1306/819A3E50-16C5-11D7-8645000102C1865D.

Ratcliffe, N.M., Stanley, R.S., Gale, M.H., Thompson, P.J., and Walsh, G.J., 2011, Bedrock geologic map of Vermont: U.S. Geological Survey Scientific Investigations Map 3184, scale 1:100,000, 3 sheets, https://doi.org/10.3133/sim3184.

Rowley, D.B., 1983, Operation of the Wilson cycle in western New England during the early Paleozoic: with emphasis on the stratigraphy, structure, and emplacement of the Taconic allochthon [Ph.D. thesis]: Albany, New York, State University of New York at Albany, 602 p.

Rowley, D.B., and Kidd, W.S.F., 1981, Stratigraphic relationships and detrital composition of the medial Ordovician flysch of western New England: Implications for the tectonic evolution of the Taconic orogeny: The Journal of Geology, v. 89, no. 2, p. 199–218, https://doi.org/10.1086/628580.

Rowley, D.B., Kidd, W.S.F., and Delano, L.L., 1979, Detailed stratigraphic and structural features of the Giddings Brook slice of the Taconic allochthon in the Granville area, *in* Friedman, G.M., ed., Guidebook for the 51st Annual Meeting of the New York State Geological Association and the 71st Annual Meeting of the New England Intercollegiate Geological Conference: Troy, New York, Rensselaer Polytechnic Institute, p. 186–242.

Shaw, W.J., 1984, Geological map of portions of Granville, Hartford, Hebron townships, Washington County, New York, and Pawlet Township, Rutland County, Vermont: http://www.atmos.albany.edu/geology/webpages/SUNYATaconicGeologicalMaps.html (August 2018).

Sleep, N.H., 1990, Monteregian hotspot track: A long-lived mantle plume: Journal of Geophysical Research, v. 95, no. B13, p. 21,983–21,990, https://doi.org/10.1029/JB095iB13p21983.

Stanley, R.S., and Ratcliffe, N.M., 1985, Tectonic synthesis of the Taconian orogeny in western New England: Geological Society of America Bulletin, v. 96, no. 10, p. 1227–1250, https://doi.org/10.1130/0016-7606(1985)96<1227:TSOTTO>2.0.CO;2.

Withjack, M.O., Schlische, R.W., and Olsen, P.E., 2012, Development of the passive margin of eastern North America: Mesozoic rifting, igneous activity, and breakup, *in* Roberts, D.G., and Bally, A.W., eds., Regional Geology and Tectonics: Phanerozoic Rift Systems and Sedimentary Basins: Amsterdam, The Netherlands, Elsevier, p. 301–335, https://doi.org/10.1016/B978-0-444-56356-9.00012-2.

Wood, D.S., 1974, Current views of the development of slaty cleavage: Annual Review of Earth and Planetary Sciences, v. 2, p. 369–401, https://doi.org/10.1146/annurev.ea.02.050174.002101.

Zen, E-an, 1972, Some revisions in the interpretation of the Taconic allochthon in west-central Vermont: Geological Society of America Bulletin, v. 83, no. 9, p. 2573–2588, https://doi.org/10.1130/0016-7606(1972)83[2573:SRITIO]2.0.CO;2.